


Paper Type: Original Article

Continuous Wavelet Transform-Based Vibration Analysis for Cavitation Detection in Centrifugal Pumps: From Incipient to Extensive Cavitation

Mansour Nikkhah Bahrami^{1*} , Natalja Osintsev²

¹ Department of Mechanical Engineering, College of Engineering, University of Tehran, Iran; mbahrami@ut.ac.ir.

² Fraunhofer-Institut für Holzforschung Wilhelm-Klauditz Institut WKI, Bienroder Weg 54 E, 38108 Brunswick, Germany; n.osintsev@gmail.com.

Citation:

Received: 17 February 2023

Revised: 22 April 2023

Accepted: 24 June 2023

Nikkhah Bahrami, M., & Osintsev, N. (2024). Continuous wavelet transform-based vibration analysis for cavitation detection in centrifugal pumps: From incipient to extensive cavitation. *Mechanical Technology and Engineering Insights*, 1(3), 132-142.


Abstract


Cavitation in centrifugal pumps causes damage, leading to poor performance, noise, vibration, and material erosion. Early prediction is important in avoiding pump breakdowns. In this study, we have used the Continuous Wavelet Transform (CWT) technique for cavitation detection at various levels based on casing vibration signals of the pump. Experiments have been done on a centrifugal pump having 10 blades (2850 rpm) in four states: normal, incipient, developed, and severe cavitation. The vibration data has been collected using an accelerometer and analyzed using the CWT method with the db9 mother wavelet function. It was observed that cavitation continuously generates scales 2 (725 Hz) and 5-10 (145-290 Hz). The CWT coefficient value for these scales rises gradually with increasing cavitation severity. Even in the presence of heavy white Gaussian noise (Signal-to-Noise Ratio (SNR) 0 dB), these scale bands can be easily identified. The proposed technique is efficient and noise resilient.

Keywords: Continuous wavelet transform, Cavitation detection, Centrifugal pump, Vibration, Condition monitoring.

1 | Introduction

In most cases, cavitation is highly dangerous and should be avoided [1], [2]. Cavitation onset in the pump system begins with transient noise that gradually becomes persistent and highly intense as the inlet pressure decreases.

 Corresponding Author: mbahrami@ut.ac.ir

 <https://doi.org/10.48313/mtei.v1i3.56>



Licensee System Analytics. This article is an open access article distributed under the terms and conditions of the Creative Commons Attribution (CC BY) license (<http://creativecommons.org/licenses/by/4.0>).

This phenomenon is also accompanied by increasing vibrations [3–5]. Cavitation arises when the local absolute pressure falls below the liquid's vapor pressure, leading to bubble formation. When the bubble moves into regions of higher pressure, it implodes, producing highly pressurized fluid jets that impact solid surfaces, resulting in vibrations, erosion, and noise [6]. Cavitation in a centrifugal pump usually starts near the impeller inlet, where the velocity is maximum, and the pressure is minimum. It causes a reduction in flow rate, a decrease in head, and deterioration of impeller blade performance [6]. Thus, detecting cavitation is important to avoid pump failures.

Over the past 20 years, various approaches have been proposed for detecting cavitation in centrifugal pumps. Alfayez et al. [1] employed Acoustic Emission (AE) technology to identify incipient cavitation and determine the Best Efficiency Point (BEP) for a 60 kW centrifugal pump, demonstrating that AE signals are highly sensitive to bubble collapse. Over the past two decades, many investigators have attempted to develop various techniques for detecting cavitation in centrifugal pumps.

Čudina and Prezelj [5] applied the approach of using frequency tones in the audible range to monitor cavitation phenomena, while later Čudina and Prezelj [3], [4] conducted a comparison study of sound pressure, underwater sound, and vibrations. The authors concluded that vibration measurement is a more practical approach that strikes an effective balance between sensitivity and technical simplicity. Measurement uncertainties in detecting cavitation phenomena were estimated by Černetič and Čudina [7] using various approaches, including frequency analysis of wide-band and discrete frequency components. Cavitation noise parameters in a centrifugal pump were analyzed experimentally using power spectral density and wavelet transform techniques by Wang et al. [8].

Al Obaidi [9], [10] studied vibration-based cavitation diagnosis techniques in time and frequency domains, proving that vibration patterns are substantially altered as cavitation progresses. Sakthivel et al. [11] employed decision trees for vibration-based fault diagnosis of monoblock centrifugal pumps, with cavitation as a possible fault.

Azizi et al. [12] focused solely on the detection of cavitation severity and proposed cavitation-related vibration indices. Cavitation was detected using vibration signal analysis by Ganeriwala and Kanakasabai [13], emphasizing the role of high-frequency components. Spectral kurtosis method for cavitation detection using vibration data was introduced by Yiakopoulos et al. [14].

Mousmoulis et al. [15] conducted an experiment that included AE, vibration monitoring, and flow visualization to investigate cavitation formation in a centrifugal pump. Li et al. [16] combined numerical, experimental, and deep learning approaches to characterize hydrodynamic performance and cavitation evolution. McKee et al. [17] proposed a vibration-based cavitation-sensitivity parameter that enables quantitative estimation of cavitation severity from spectral and statistical vibration characteristics.

Among these techniques, vibration analysis has been found interesting due to its stability and insensitivity to environmental changes, as well as its ease of measurement using industrial accelerometers [3–5]. Despite being unstable (i.e., nonstationary), vibration signal analysis in a centrifugal pump is relatively simple, since cavity bubble collapse occurs in a broad-band manner and involves transient phenomena. This aspect cannot be captured using conventional spectral analysis techniques like the FFT, which suffer from the time-average problem. STFT, on the other hand, is used to overcome such a problem but is subject to a constant trade-off between time and frequency. Continuous Wavelet Transform (CWT) provides an ideal solution to such issues because multi-resolution analysis allows the use of a small window at higher frequencies (time resolution) and a larger window at lower frequencies (frequency resolution) [8], [11], [12].

In this work, vibration data are obtained for four operating conditions of the centrifugal pump: normal operation, early-stage cavitation, mature cavitation, and severe cavitation. The CWT technique is implemented using the db9 mother wavelet, and the scales of interest are determined, which are strongly affected by cavitation in the rotor flow. In addition, a simulation of the effect of white Gaussian noise is performed.

2 | Experimental Setup and Data Acquisition

An experimental setup was developed as a closed-loop circuit to produce controlled cavitation conditions (*Fig. 1*). The test pump consists of a 10-blade centrifugal pump driven by a 2850 rpm electric motor (shaft rotation frequency = approx. 50 Hz; Blade Passing Frequency (BPF)= approx. 500 Hz). A piezoelectric accelerometer (0.5 Hz–20 kHz) was placed in proximity to the pump outlet, where bubbles collapse under high pressure, generating maximum vibrations. A magnetic clamp was used to ensure proper sensor mounting. Signals were collected at 32 L/min flow using an A/D converter board (4 channels, ±5 V; max output frequency 10 kHz; anti-aliasing filter) with a sampling frequency of 4096 Hz, yielding an effective sampling frequency of 2048 Hz after the anti-aliasing filter.



Fig. 1. Schematic diagram of the experimental setup.

Four distinct modes of operation were identified from the observations and sounds:

- I. Normal condition: No cavitation, smooth functioning, no bubble collapse sound.
- II. Incipient cavitation: Emergence of bubble collapse sound for the first time, weak intensity, no performance decrease.
- III. Developed cavitation: Continuous sound, increased vibrations, and performance reduction start.
- IV. Extensive cavitation: Well-developed cavitation, heavy vibrations, noise, and a decrease in flow rate and head.

A vibration signal captured in the time domain by an accelerometer when it is functioning normally is shown in *Fig. 2* below.

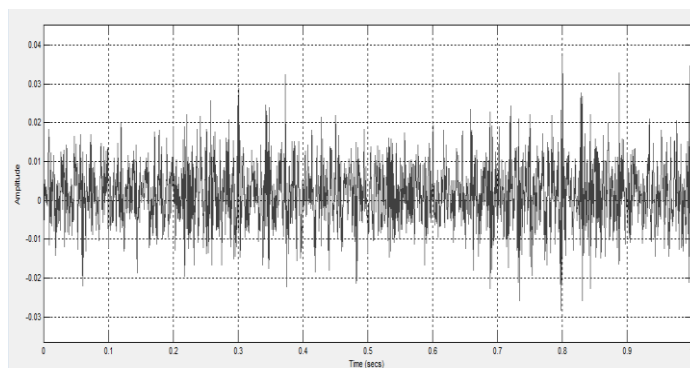


Fig. 2. Time-domain vibration signal acquired from the accelerometer under normal conditions.

3 | Continuous Wavelet Transform Theory

The CWT is an approach that uses time-frequency analysis to represent signals using wavelets. The definition of the CWT is provided below.

$$\text{CWT}_x^\psi(\tau, s) = \Psi_x^\psi(\tau, s) = \frac{1}{\sqrt{|s|}} \int_{-\infty}^{+\infty} x(t) \psi^* \left(\frac{t - \tau}{s} \right) dt. \quad (1)$$

Here, $x(t)$ represents the signal, $\psi(t)$ denotes the mother wavelet, s represents the scaling factor, and τ is the translation parameter. In this work, db9 (Daubechies 9) was used as the mother wavelet, which has good localization characteristics and has been previously applied successfully for fault detection in mechanical systems [8], [12]. Scale s is inversely proportional to frequency; small scales are associated with higher frequencies (better time resolution), while larger scales are associated with lower frequencies (better frequency resolution). The equation relating scale s and the corresponding frequency f is:

$$f = \frac{f_c}{s \Delta t}, \quad (2)$$

where f_c is the central frequency of the mother wavelet (for db9, $f_c \approx 0.714$ Hz for each sampling time interval), s is the scale, and Δt is the sampling interval. For a sampling rate of 2048 Hz, $\Delta t = 1/2048 \approx 0.000488$.

4 | Results and Discussion

4.1 | Three-Dimensional Continuous Wavelet Transform Scalograms

The three-dimensional CWT scalograms for each of the four modes of operation of the centrifugal pump, viz., normal, incipient, developed, and extensive cavitation, are illustrated in *Figs. 3–6*. In the scalogram plots, the horizontal axis corresponds to time, and the vertical axis represents wavelet scale (1–50). The color intensity indicates the values of the CWT coefficients.

In the pump's normal operating mode (*Fig. 3*), the CWT coefficients have very small values across almost all scales. The only activity identified is low-intensity at the higher scales (40–50), corresponding to the low-frequency range (36–45 Hz) and representing shaft rotation. There is no concentration of energy for scales lower than 15.

With the onset of cavitation (*Fig. 4*), distinct energetic regions emerge at scale 2 (≈ 725 Hz) and within scales 5–10 (≈ 145 –290 Hz). Unlike the normal condition, these regions appear intermittently along the time axis, indicating sporadic bubble collapse events characteristic of incipient cavitation. The transient nature of these localized structures demonstrates CWT's ability to detect cavitation signatures before any measurable degradation in hydraulic performance.

As cavitation develops further (*Fig. 5*), the magnitude of the wavelet coefficients at scales 2 and 5–10 increases substantially. The energetic structures become wider and more continuous in time, indicating a higher frequency of bubble collapse events and stronger transient pressure fluctuations. In addition, weak activity is observed at intermediate scales between 15 and 25, suggesting a gradual spread of vibration energy into adjacent frequency bands.

In the case of extensive cavitation (*Fig. 6*), there is continuous high wavelet activity from scale 2 to 15. In contrast, the background energy level at higher scales also rises. The earlier localized energy zones become a near-continuous broad-band feature, indicating that the vibrations are now mainly caused by cavitation across a broad spectrum of frequencies.

This broad-band stimulation is characteristic of full cavitation, in which the random collapse of bubble clusters of various sizes results in highly non-stationary vibrations. The highest coefficient value obtained under this scenario is about an order of magnitude higher than in the normal operation scenario.

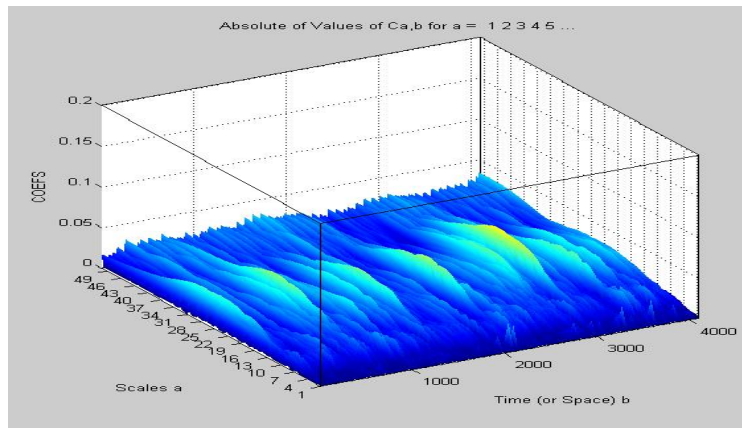


Fig. 3. Three-dimensional CWT scalogram for normal condition.

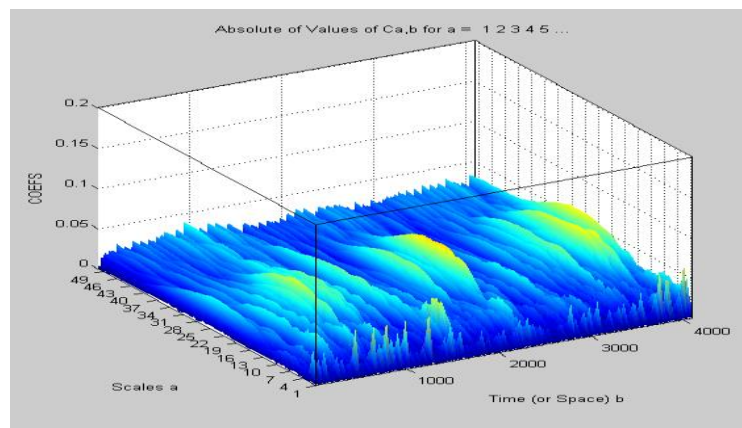


Fig. 4. Three-dimensional CWT scalogram for incipient cavitation.

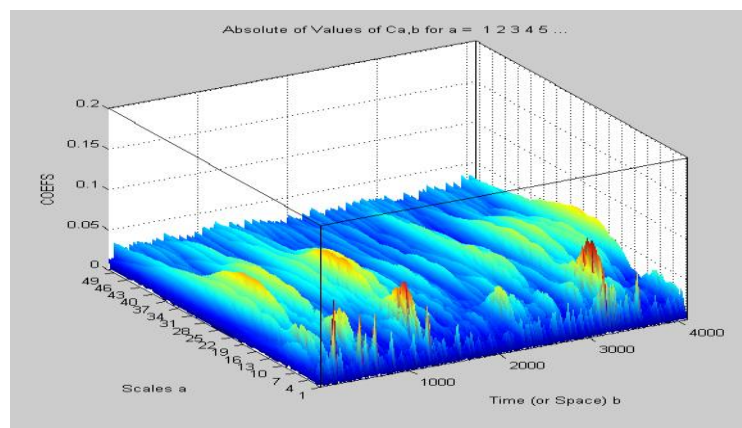


Fig. 5. Three-dimensional CWT scalogram for developed cavitation.

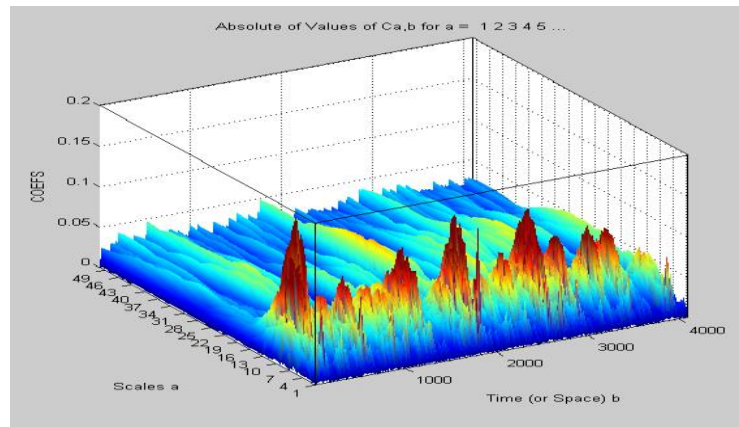


Fig. 6. Three-dimensional CWT scalogram for extensive cavitation.

4.2 | Two-Dimensional Scale–Time Representations

To better visualize the scales sensitive to cavitation, the same CWT results are depicted in two dimensions as contours in *Figs. 7-10*. Here, time is plotted along the horizontal axis, the scale along the vertical axis, and the coefficient value indicated by color intensity. Compared with three-dimensional scalograms, the two-dimensional representation allows better detection of persistent energetic bands arising from cavitation.

In *Fig. 7*, which represents the case where there is no cavitation present, no distinct horizontal bands are found. Weak, sparse low-energy bands appear only at scales greater than 35.

When incipient cavitation begins (*Fig. 8*), clear horizontal bands emerge at scale 2 and scales between 5 and 10. The horizontal bands have intermittent interruptions, indicating that cavitation is a temporary process. The energetic bands detected here indicate that certain scales are more sensitive to cavitation than others.

With increased cavitation intensity (*Fig. 9*), the high-energy bands from scale 2 to scale 10 become denser and more persistent over time. Also, some new low-energy features appear at scales 12-18. It is shown that the energy of cavitation moves increasingly towards adjacent scales as bubble collapse becomes more intensive.

During intense cavitation (*Fig. 10*), the separated high-energy bands coalesce into a single band spanning scales 2-15. Also, higher levels of background noise start appearing at even higher scales (>30). This phenomenon shows the existence of broad-band stochastic vibrations.

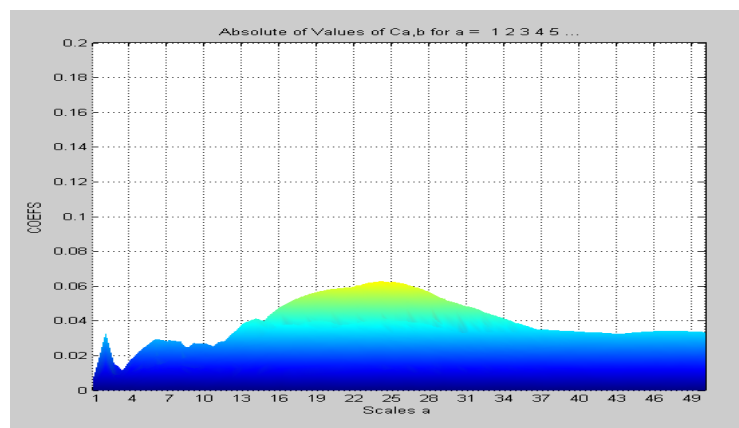


Fig. 7. Two-dimensional scale-parameter CWT representation for normal condition.

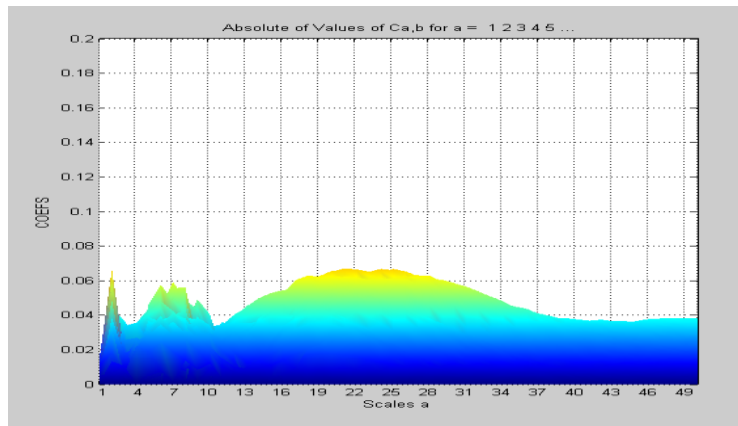


Fig. 8. Two-dimensional scale-parameter CWT representation for incipient cavitation.

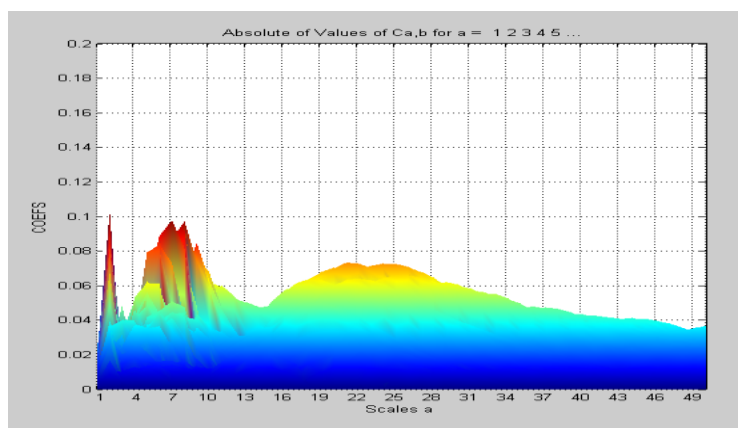


Fig. 9. Two-dimensional scale-parameter CWT representation for developed cavitation.

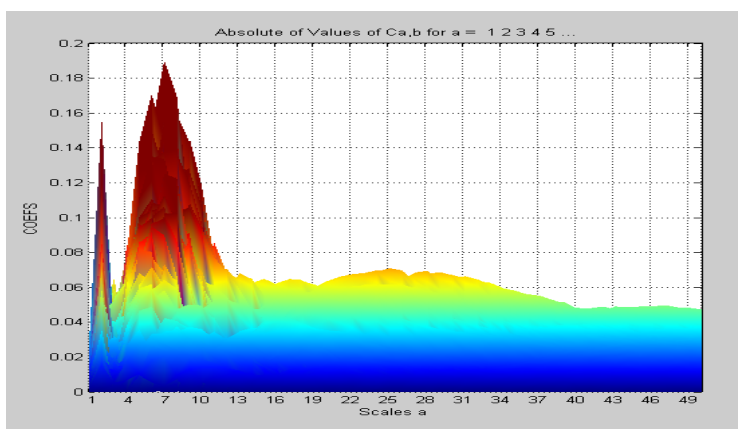


Fig. 10. Two-dimensional scale-parameter CWT representation for extensive cavitation.

4.3 | Frequency Interpretation and Physical Mechanisms

The relationship between wavelet scale and frequency was established based on the scale-frequency conversion presented in Section 3:

$$F_a = \frac{F_c}{a \cdot \Delta}, \tag{2}$$

where F_a refers to the equivalent frequency, F_c represents the central frequency of the mother wavelet, Δ stands for the sampling frequency, and a refers to the wavelet scale. Using this relation, the scales that respond most effectively to cavitation events are those whose corresponding frequencies lie within the following ranges:

- I. Scale 2 corresponds to 725 Hz
- II. Scales 5 to 10 correspond to 145 to 290 Hz

The mid-frequency range of 145 to 290 Hz appears to be linked to cavitation bubble oscillation and pressure pulsations within the pump volute. This frequency range is consistent with that reported in previous studies examining cavitation in centrifugal pumps.

On the other hand, the 725 Hz high-frequency component may be attributed to liquid microjets generated by the collapse of cavitation bubbles adjacent to solid surfaces. It is noteworthy that the BPF, approximately 500 Hz for the present pump, does not appear as a dominant feature in the CWT scalograms. Unlike deterministic mechanical excitations associated with rotational harmonics, cavitation gives rise to highly transient, stochastic vibrations across multiple frequency ranges. Thus, the CWT focuses on the identification of transient structures associated with cavitation rather than on the amplification of periodic mechanical excitations. Such a trait greatly increases the precision of cavitation detection under different operating and rotation rates.

4.4 | Noise Robustness Analysis

To test the performance of the proposed algorithm in a realistic industrial setting, white Gaussian noise with an amplitude similar to that of the initial signal was added to the obtained data. The latter implies a very noisy environment with a Signal-to-Noise Ratio (SNR) of 0 dB.

About the noisy normal condition (see *Fig. 11*), no energy concentration occurs in the form of organized bands; instead, the wavelet coefficients remain distributed randomly, forming a scalogram characterized by small intensity throughout all scales. Nevertheless, even in the case of a severely contaminated signal, cavitation-related bands at scale 2 and scales 5-10 become detectable during incipient cavitation (see *Fig. 12*).

With increasing cavitation intensity (*Fig. 13*), energetic peaks become more distinct as the vibration energy induced by cavitation exceeds the noise-induced energy. For extensive cavitation (*Fig. 14*), the broad-band energetic peak from scales 2 to 15 remains very prominent, similar to the noise-free case.

The robustness of the suggested method lies in the CWT's intrinsic ability to detect transient energy localized at certain scales. In contrast, stationary noise is spread across the entire range of scales. Therefore, structures associated with cavitation will still be identifiable even in the presence of strong noise. Sakthivel and Mousmoulis have reported similar robustness features for wavelet-based fault diagnosis.

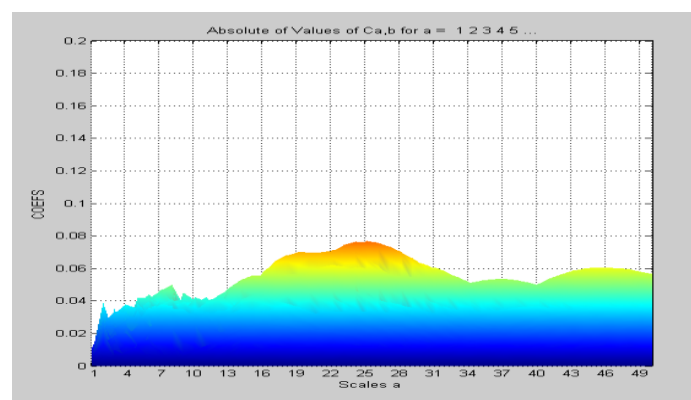


Fig. 11. Two-dimensional CWT for a noisy signal under normal conditions.

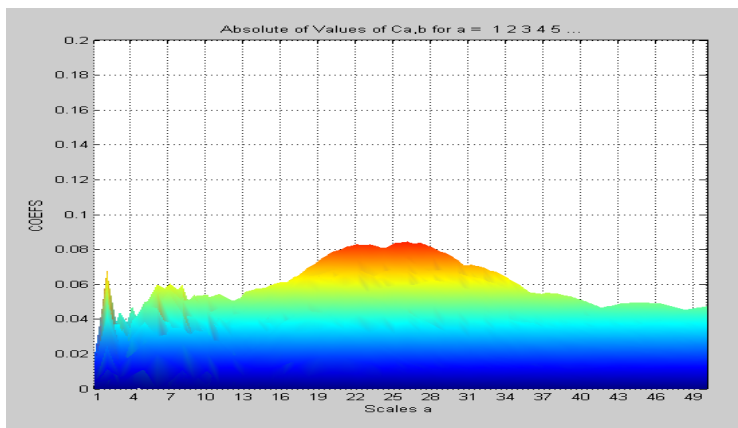


Fig. 12. Two-dimensional CWT for a noisy signal under incipient cavitation.

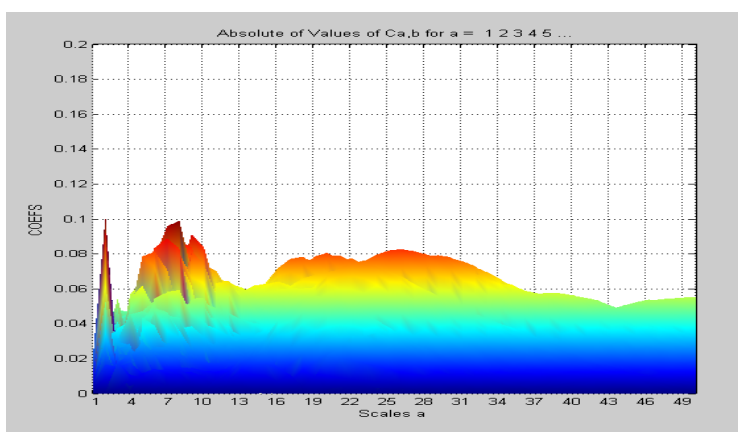


Fig. 13. Two-dimensional CWT for a noisy signal under developed cavitation.

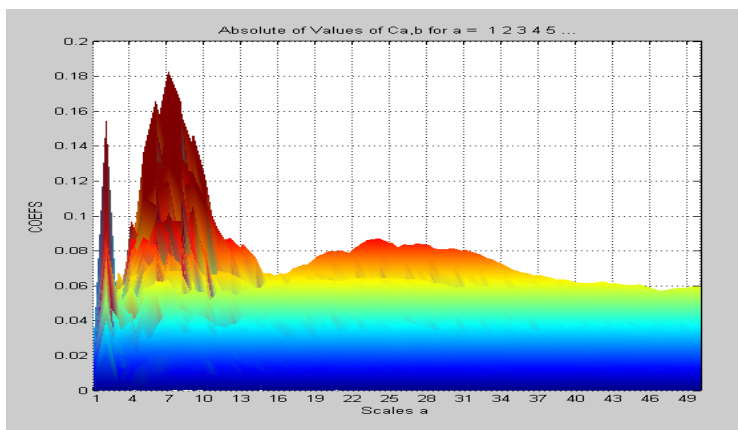


Fig. 14. Two-dimensional CWT for a noisy signal under extensive cavitation.

5 | Conclusion

The paper assessed the feasibility of the CWT for cavitation detection in a centrifugal pump using vibration signals. Key conclusions drawn are:

- I. Sensitivities to specific scales: Cavitation is found to consistently excite scales 2 (≈ 725 Hz) and 5–10 (≈ 145 –290 Hz) in the CWT analysis of pump casing vibration signals.
- II. Monotonic progression: The magnitude of CWT coefficients of the aforementioned scales progressively increases with increasing cavitation severity—normal, incipient, developed, and extensive cavitations. This

phenomenon makes the method suitable not only for cavitation detection but also for estimating cavitation severity.

III. Resilience to noise: Despite the presence of a 0 dB signal-to-noise ratio white Gaussian noise, where noise and signal have equal amplitudes, the sensitivities of these scales remain detectable. This phenomenon confirms the feasibility of the proposed technique for practical industrial applications.

IV. Feasibility: Real-time monitoring of these scales using a simple thresholding algorithm is a reliable, low-cost cavitation warning system that requires only a basic accelerometer and an average sample frequency.

Further research can be conducted using different mother wavelets such as Morlet, Symlet, and Coiflet. Moreover, the combination of CWT and Machine Learning (ML) models, such as Convolution Neural Networks (CNNs), can be used for cavitation detection and classification.

Conflict of Interest

The authors declare that there is no conflict of interest regarding the publication of this article.

Data Availability

All data generated or analyzed during this study are included in this published article. No additional data are available.

Funding

This research did not receive any specific grant from funding agencies in the public, commercial, or not-for-profit sectors.

References

- [1] Alfayez, L., Mba, D., & Dyson, G. (2005). The application of acoustic emission for detecting incipient cavitation and the best efficiency point of a 60kW centrifugal pump: Case study. *NDT & e international*, 38(5), 354–358. <https://doi.org/10.1016/j.ndteint.2004.10.002>
- [2] Senocak, I. (2002). *A computational methodology for the simulation of turbulent cavitating flows*. University of Florida. <https://search.proquest.com/openview/c84fc5fe43ade467872f39b37a4640bd/1?pq-origsite=gscholar&cbl=18750&diss=y>
- [3] Čudina, M., & Prezelj, J. (2009). Detection of cavitation in situ operation of kinetic pumps: Effect of cavitation on the characteristic discrete frequency component. *Applied acoustics*, 70(9), 1175–1182. <https://doi.org/10.1016/j.apacoust.2009.04.001>
- [4] Čudina, M., & Prezelj, J. (2009). Detection of cavitation in operation of kinetic pumps. Use of discrete frequency tone in audible spectra. *Applied acoustics*, 70(4), 540–546. <https://doi.org/10.1016/j.apacoust.2008.07.005>
- [5] Čudina, M., & Prezelj, J. (2008). Use of audible sound for safe operation of kinetic pumps. *International journal of mechanical sciences*, 50(9), 1335–1343. <https://doi.org/10.1016/j.ijmecsci.2008.07.012>
- [6] Buckland, H. C., Masters, I., Orme, J. A. C., & Baker, T. (2013). Cavitation inception and simulation in blade element momentum theory for modelling tidal stream turbines. *Proceedings of the institution of mechanical engineers, part a: Journal of power and energy*, 227(4), 479–485. <https://doi.org/10.1177/0957650913477093>
- [7] Černetič, J., & Čudina, M. (2011). Estimating uncertainty of measurements for cavitation detection in a centrifugal pump. *Measurement*, 44(7), 1293–1299. <https://doi.org/10.1016/j.measurement.2011.03.023>
- [8] Dong-wei, W., Wei-dong, W., Jia-jun, H., Wei-guo, Z., & Lai, L. (2023). Experimental study of cavitation noise characteristics in a centrifugal pump based on power spectral density and wavelet transform. *Flow measurement and instrumentation*, 94, 102481. <https://doi.org/10.1016/j.flowmeasinst.2023.102481>

- [9] Al-Obaidi, A. R., & Mishra, R. (2020). Experimental investigation of the effect of air injection on performance and detection of cavitation in the centrifugal pump based on vibration technique. *Arabian journal for science and engineering*, 45(7), 5657–5671. <https://doi.org/10.1007/s13369-020-04509-3>
- [10] Al-Obaidi, A. R. (2020). Detection of cavitation phenomenon within a centrifugal pump based on vibration analysis technique in both time and frequency domains. *Experimental techniques*, 44(3), 329–347. <https://doi.org/10.1007/s40799-020-00362-z>
- [11] Sakthivel, N. R., Sugumaran, V., & Babudevasenapati, S. (2010). Vibration based fault diagnosis of monoblock centrifugal pump using decision tree. *Expert systems with applications*, 37(6), 4040–4049. <https://doi.org/10.1016/j.eswa.2009.10.002>
- [12] Azizi, R., Hajnayeb, A., Ghanbarzadeh, A., & Changizian, M. (2018). Cavitation severity detection in centrifugal pumps. *Advances in technical diagnostics* (pp. 47–55). Cham: Springer International Publishing. https://doi.org/10.1007/978-3-319-62042-8_4
- [13] Ganeriwala (Suri), S. N., & Kanakasabai (Vetri), V. (2011). Using vibration signatures analysis to detect cavitation in centrifugal pumps. *Rotating machinery, structural health monitoring, shock and vibration, volume 5* (pp. 499–507). New York, NY: Springer New York. https://doi.org/10.1007/978-1-4419-9428-8_41
- [14] Mousmoulis, G., Yiakopoulos, C., Aggidis, G., Antoniadis, I., & Anagnostopoulos, I. (2021). Application of Spectral Kurtosis on vibration signals for the detection of cavitation in centrifugal pumps. *Applied acoustics*, 182, 108289. <https://doi.org/10.1016/j.apacoust.2021.108289>
- [15] Mousmoulis, G., Karlsen-Davies, N., Aggidis, G., Anagnostopoulos, I., & Papantonis, D. (2019). Experimental analysis of cavitation in a centrifugal pump using acoustic emission, vibration measurements and flow visualization. *European journal of mechanics - b/fluids*, 75, 300–311. <https://doi.org/10.1016/j.euromechflu.2018.10.015>
- [16] Li, G., Sun, H., He, J., Ding, X., Zhu, W., Qin, C., ... & Guo, Y. (2024). Deep learning, numerical, and experimental methods to reveal hydrodynamics performance and cavitation development in centrifugal pump. *Expert systems with applications*, 237, 121604. <https://doi.org/10.1016/j.eswa.2023.121604>
- [17] McKee, K. K., Forbes, G. L., Mazhar, I., Entwistle, R., Hodkiewicz, M., & Howard, I. (2015). A vibration cavitation sensitivity parameter based on spectral and statistical methods. *Expert systems with applications*, 42(1), 67–78. <https://doi.org/10.1016/j.eswa.2014.07.029>